

Supporting Information

Quasi-perpetual discharge behaviour in p-type Ge-air battery

Joey D. Ocon^a, Jin Won Kim^a, Graniel Harne A. Abrenica^a, Jae Kwang Lee^b, and
Jaeyoung Lee^{*,a,b}

^aElectrochemical Reaction and Technology Laboratory (ERTL), School of Environmental Science and Engineering, Gwangju
Institute of Science and Technology, Gwangju 500-712, South Korea.

^bErtl Center for Electrochemistry and Catalysis, Research Institute for Solar and Sustainable Energies (RISE), Gwangju Institute
of Science and Technology, Gwangju 500-712, South Korea.

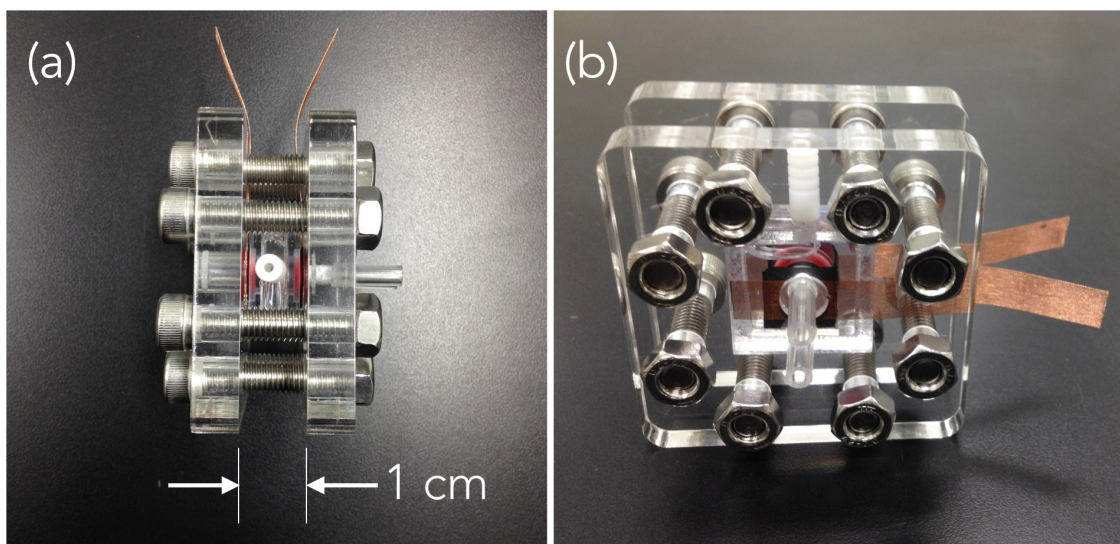


Figure S1. Photographs of the semiconductor-air cell in (a) top and (b) side views.

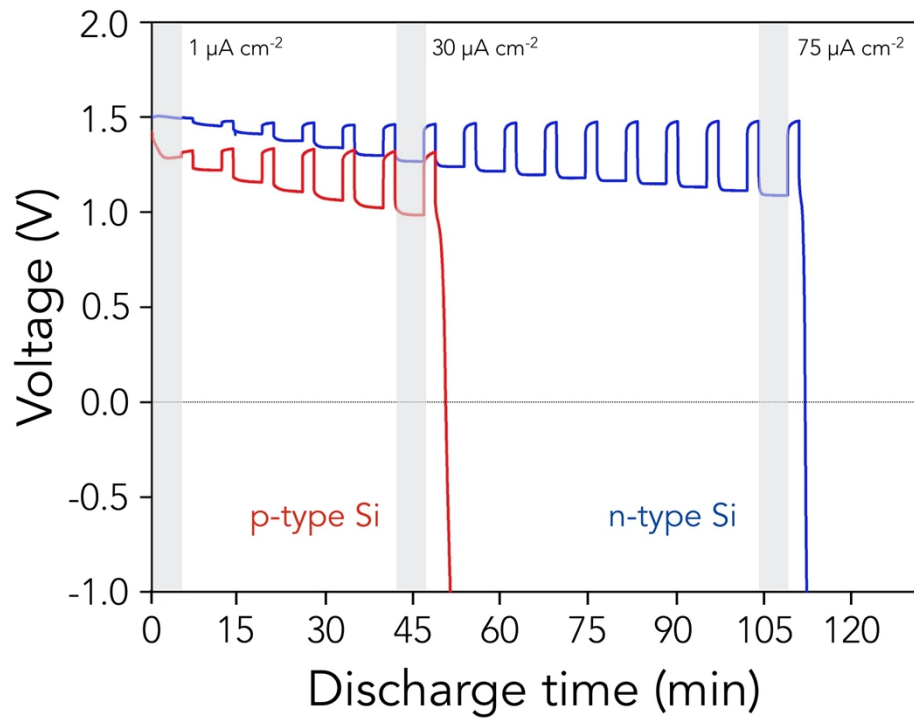


Figure S2. Dynamic step discharge response of heavily doped flat Si anodes at various current drains.

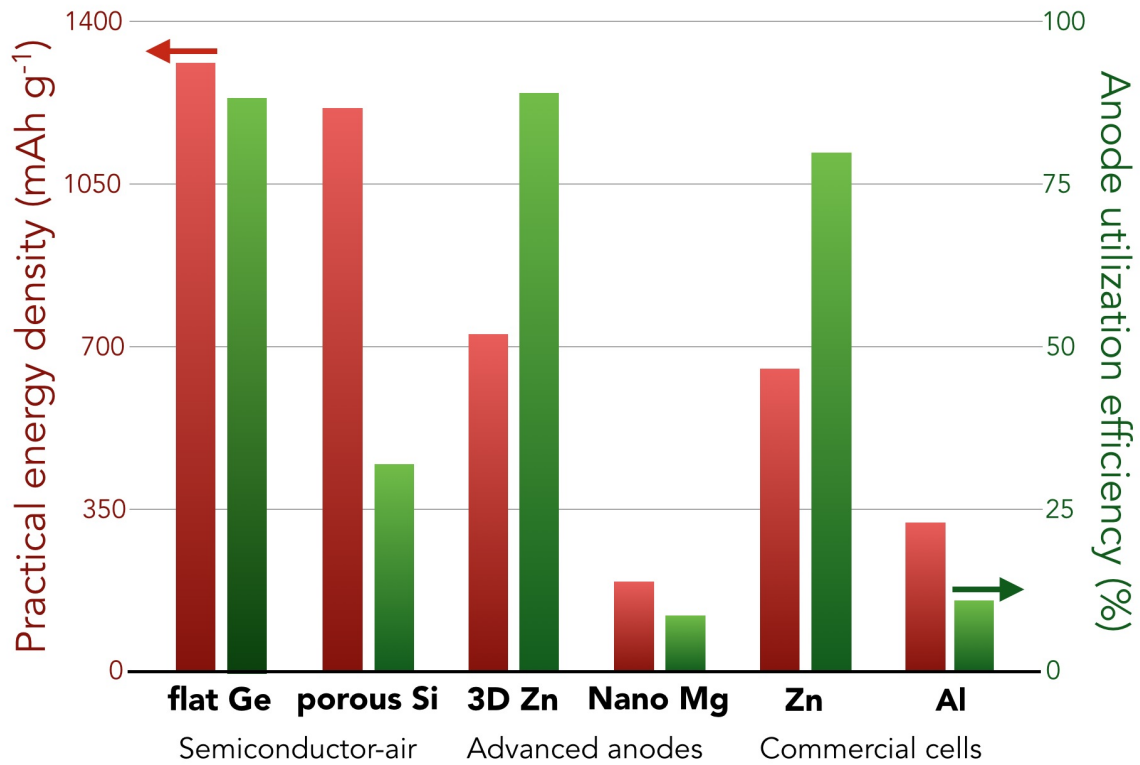


Figure S3. Comparison of the practical energy density and anode utilization efficiency of different metal-air chemistries, emphasizing the advantages of p-type Ge-air cell in terms of high practical energy capacity and anode utilization.

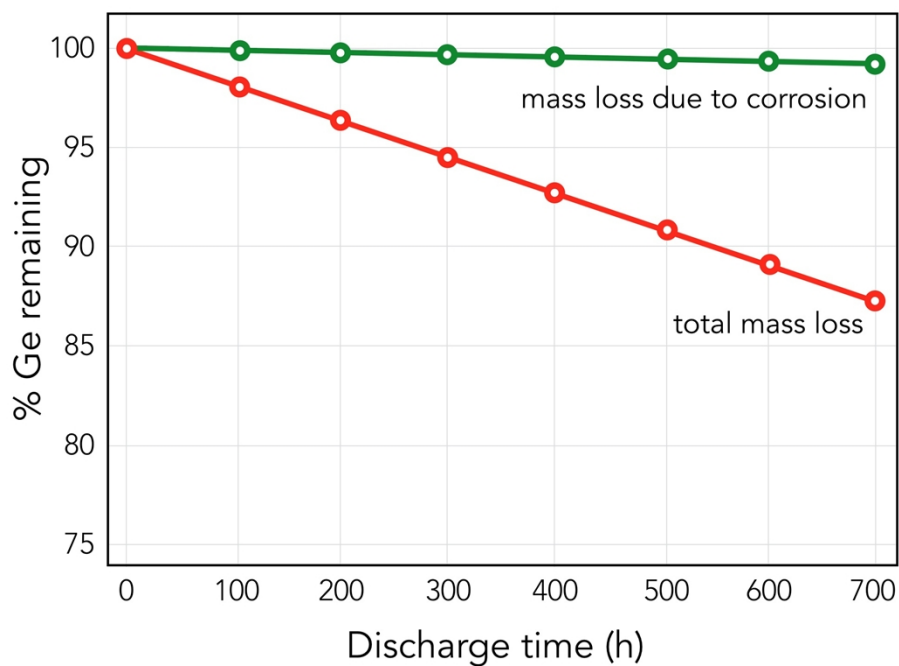


Figure S4. Experimental mass loss during long-term discharge of p-type Ge-air cell and the computed mass loss due to the self-discharge, using an average corrosion current of $5.02 \mu\text{A cm}^{-2}$ for p-type Ge from the corrosion experiments. The mass loss curves are assumed to be linear with respect to the discharge time.

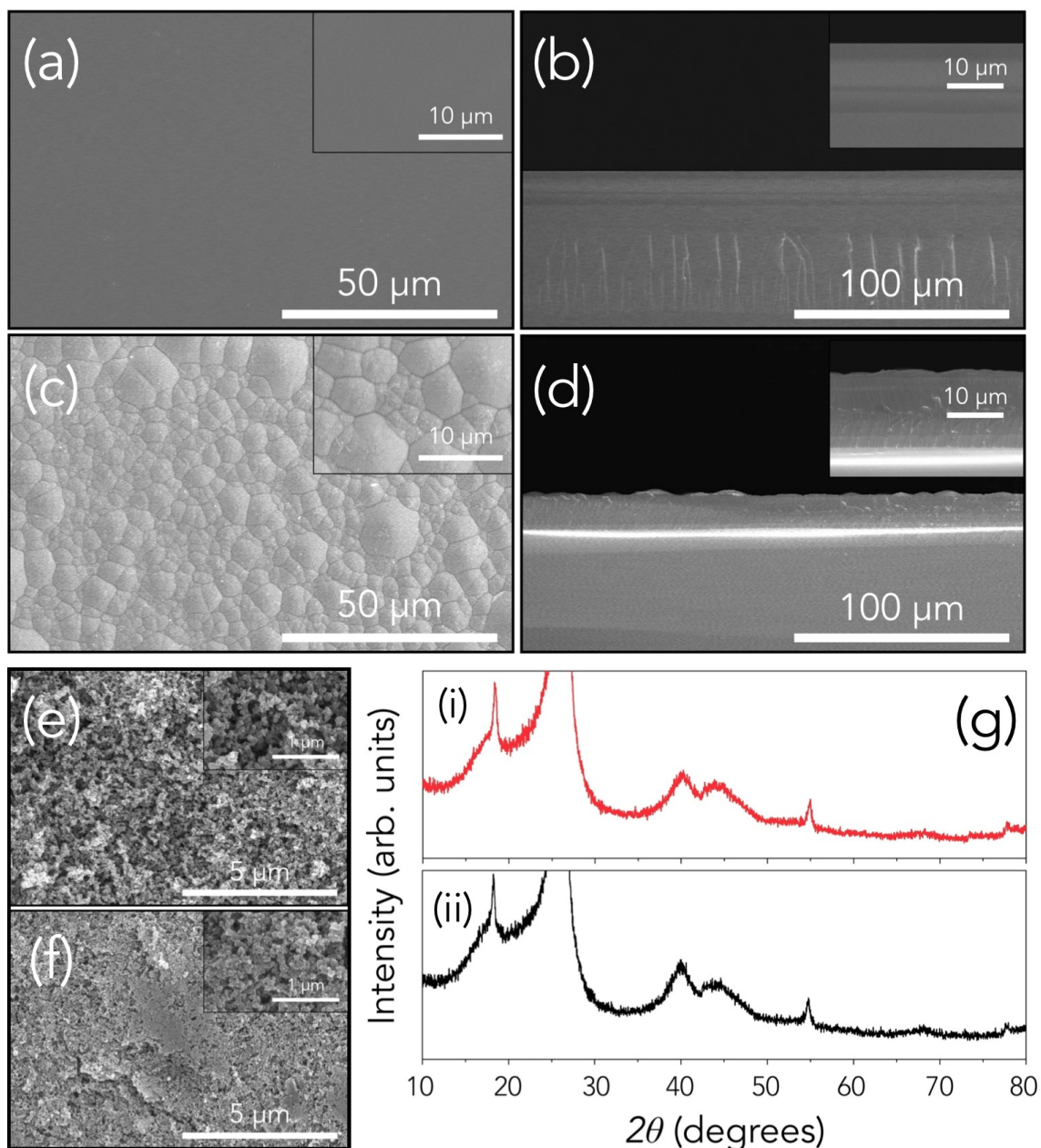


Figure S5. (a) Plain and (b) cross section SEM images of the pristine p-type Ge anode before battery discharge. (c) Plain and (d) cross section SEM images of the post-discharge p-type Ge anode, showing the change in surface morphology. SEM images of the cathode (e) before and (f) after long-term discharge. (g) X-ray diffractograms of the cathode (i) before and (ii) after long-term discharge, showing that the cathode remained the same.

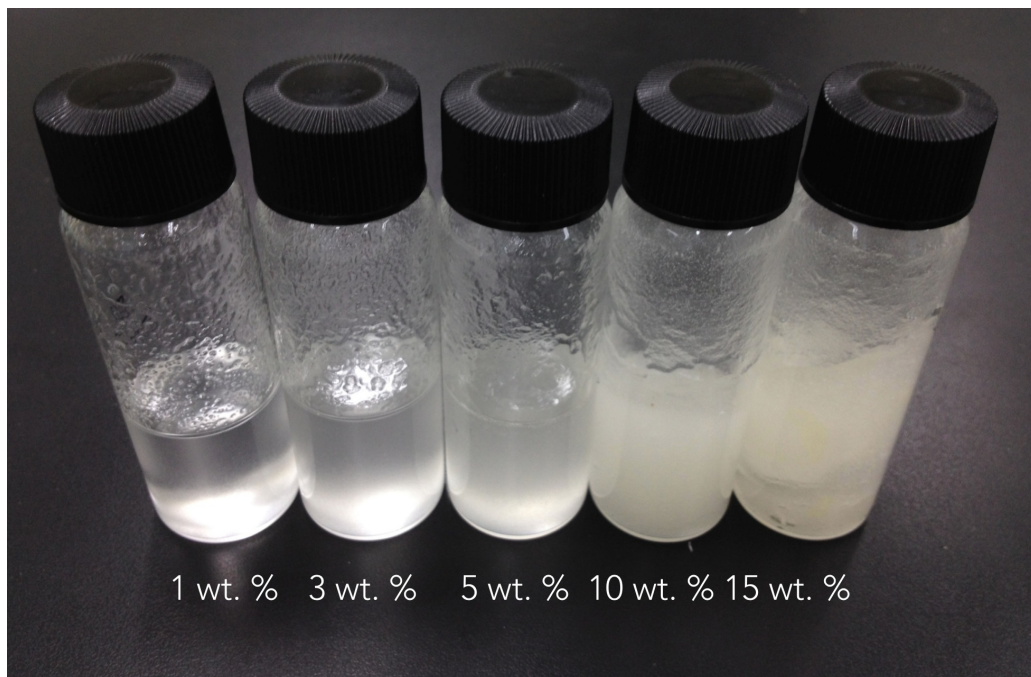


Figure S6. Image of different gelled KOH electrolytes with varying gelling agent (CMC) amounts.